Steady-state kinetics of solitary bachtrachotoxin-treated sodium channels

Kinetics on a bounded continuum of polymer conformations

Kenneth A. Rubinson

The Five Oaks Research Institute, Cincinnati, Ohio 45238-5157; and Department of Physiology and Biophysics, University of Cincinnati, School of Medicine, Cincinnati, Ohio 45287-0576

ABSTRACT The underlying principles of the kinetics and equilibrium of a solitary sodium channel in the steady state are examined. Both the open and closed kinetics are postulated to result from round-trip excursions from a transition region that separates the openable and closed forms. Exponential behavior of the kinetics can have origins different from small-molecule systems. These differences suggest that the probability density functions (PDFs) that describe the time dependences of the open and closed forms arise from a distribution of rate constants. The distribution is likely to arise from a thermal modulation of the channel structure, and this provides a physical basis for the following three-variable equation:

$$\rho(t) = A_0 \exp\left[-\left(\bar{k}t - \frac{\sigma^2 t^2}{2}\right)\right] \operatorname{erfc}\left[\frac{1}{\sqrt{2}}\left(\sigma t - \frac{\bar{k}}{\sigma}\right)\right]$$

Here, A_0 is a scaling term, $\bar{k}$ is the mean rate constant, and σ quantifies the Gaussian spread for the contributions of a range of effective rate constants. The maximum contribution is made by $\bar{k}$, with rates faster and slower contributing less. (When σ, the standard deviation of the spread, goes to zero, then $\rho(t) = A_0\, e^{-kt}$.) The equation is applied to the single-channel steady-state probability density functions for batrachotoxin-treated sodium channels (1986. Keller et al. *J. Gen. Physiol.* 88: 1–23). The following characteristics are found: (*a*) The data for both open and closed forms of the channel are fit well with the above equation, which represents a Gaussian distribution of first-order rate processes. (*b*) The simple relationship

$$K_{eq} = \frac{\bar{k}_{opening}}{\bar{k}_{closing}},$$

holds for the mean effective rate constants. Or, equivalently stated, the values of P_{open} calculated from the $\bar{k}$ values closely agree with the P_{open} values found directly from the PDF data. (*c*) In agreement with the known behavior of voltage-dependent rate constants, the voltage dependences of the mean effective rate constants for the opening and closing of the channel are equal and opposite over the voltage range studied. That is,

$$\frac{d \log \bar{k}_{opening}}{dV} = -\frac{d \log \bar{k}_{closing}}{dV}.$$

"Bursts" are related to the well-known cage effect of solution chemistry.

INTRODUCTION

Attributes of a continuum of conformations and round-trip kinetics

Why choose a bounded continuum of conformations?

A description of the channel latencies seen in voltage clamp experiments indicate that the molecular motions of sodium channels are usefully characterized with a continuum of conformational forms (Rubinson, 1978, 1982, 1986*a*, *b*). The latency distribution appears to behave as expected for a conformational change that occurs over a fixed distance and with the motion driven by the applied potential: i.e., simultaneous migration in the electric field and spreading by thermal diffusion. The diffusion coefficient for the process agrees with those found by photobleaching and recovery for proteins in membranes and by other techniques for macromolecules. As a result, the continuum interpretation provides a useful link between the electrophysiological measurements and measurements by other experimental techniques.

Other arguments for the use of a continuum lie with the descriptive chemistry for polymeric species such as a sodium channel. Such molecules exhibit a large number of conformations spread over a wide range of structures

0006-3495/92/02/463/17 $2.00

of approximately equal energy (Clementi, 1985; Dickinson, 1985; Gol'danskii et al., 1986; Millhauser, 1990). For the sodium channel, we can be more specific. The primary structure of the protein indicates that it is likely that relatively stiff helices are connected by short random coils (Noda et al., 1984), and these coils are likely to behave as flexible molecular springs that allow a relatively broad range of structures that are essentially energetically degenerate. Further, polymers tend to have structural changes due to bond rotations, which are not separated by large activation energies (Flory, 1969). As a result, even defining conformational states in energy terms is then impractical (Widom, 1965, 1971), and a continuum is again suggested to make the system's description tractable. Both the necessity to interpret the possible structures as forming a continuum of states and the relatively narrow range of structures expected for an open channel (see below) now seem to have been accepted by a number of workers (Liebovitch et al., 1987; Croxton, 1988; Läuger, 1988; Millhauser et al., 1988; Liebovitch, 1989; Eisenberg, 1990; Millhauser, 1990).

The structural continuum consists, nevertheless, of a limited number of conformations. For example, denatured protein structures need not be considered in the kinetics and equilibrium of the fluctuating channel. We say that the conformational range is bounded. As evidence, note that if the channel's charged groups were not bounded by physical restraints, then after the channel conformation changes in response to the applied field the groups might simply move off into the bulk solution surrounding the channel rather than return eventually to their original positions.

Rate and equilibrium constants must be average properties

The equilibrium and kinetics of chemical changes deal primarily with averages of a large number of events occurring in an average environment. That is, two averages are involved for each reaction step—when one chemical species changes to another species. First, to get a precise macroscopic measurement one must obtain a correct average of a large enough number of individual molecular events. Only a few experimental methods can record the individual molecular chemical events that eventually collectively comprise the macroscopic average. Recording the currents from individual ion channels is one of the few, and the strengths and weaknesses of the methods of averaging to the ensemble average are well understood. Second, one must obtain an average over the variations that occur within the molecular environment so that, in effect, a single distinct process is observed. However, as will be shown, the measurements made from a single sodium channel under quasi-equilibrium conditions do not inherently provide an averaging of the molecular environment. We must arithmetically average the data ourselves to obtain the ensemble average rate.

Short-range nature of the open-channel conformations and the choice of reference conformation

The formation of an open ion channel that allows facile ion passage through a membrane produces a low–chemical–potential path that does not exist when the channel is closed. The change in resistance to ion permeation is presumably due to differences in some energies of interaction of the permeant ions with structures of the channel. Only one of these interactions need differ by a few times k_BT to cause the difference in conduction, and energy changes of this magnitude in chemical bonding occur over distances small on the atomic scale. For instance, a chemical bond is made or broken over a distance of less than 0.2 Å, and a molecular structure that produces a "best fit" minimum binding energy to a substrate or ligand only can vary over that small range (Jencks, 1969; Bruice, 1970; Dunitz, 1979; Dickinson, 1985). Thus, we infer that the optimum conformational range of an open channel is likely to be spatially narrow.

In a similar way, we can estimate the distance associated with the transition region between openable and closed forms of the channel; it is expected to be no greater in extent than the distance of chemical bond formation (although a number of sites moving such distances may be involved). This transition region is traversed rapidly, which corresponds to the rapid rate at which the ion current is switched between low and high levels. Because of its sharpness and its close relationship to the experimentally measured current changes, we choose this transition region between the closed and openable forms as both the spatial and temporal reference points to study the molecular basis of the channel kinetics. It is interesting that within a channel's broad and energetically relatively flat continuum of conformations, the ability to register the position of conversion between open and closed forms at the transition region may be the most precise indicator of a polymer conformation that exists.

Round trip kinetics and its time dependence

To analyze the time dependence of the open and closed times, let us consider that some chemical group of the channel migrates within the bounded continuum and that its location determines whether the channel is openable or closed. The migration is represented as being effectively one-dimensional (see below).

One key to the analysis of the kinetics is to recognize

that the repeated arrival at the transition structure involves a round–trip path in both the range of open and range of closed conformations. To relate the channel's molecular motions to the experimental probability density functions (PDFs) we now ask, What is the expected time dependence of these repeated arrivals at the transition region? The answer to this question has been derived (Feller, 1968) once we recognize that the repeated arrivals are all so-called *first returns* to the transition region. In effect, the time is reset to zero after each arrival. Feller (1968) shows that at early times, when the migrating group does not have time to reach the boundary and return, the PDF for first returns to the transition region is expected to have a time dependence $t^{-3/2}$ in the absence of a bias field. More detailed arguments for this result are presented in Appendix II.

At long times, when the migrating group has time to reach the boundary to migration and subsequently return to the transition region, the $t^{-3/2}$ behavior passes over to an exponential decay. The origins of this exponential behavior are described next.

Origins of exponential behavior on the bounded continuum differ from small-molecule kinetics

The most common statistical interpretation of exponential, first-order kinetics is, in essence, as a Poisson distribution. Poisson statistics in this context is an approximation to the Binomial distribution describing the occurrence of unlikely events within a large number of trials (Canavos, 1984). The chemical interpretation that parallels the Poisson statistics applies to the formation and breaking of bonds and to the interconversions of conformational structures. This chemical interpretation says that the large number of trials results from a vibration within a potential well; the unlikely event is the arrival at and passage through a specific structure and energy state called the activated state (Laidler, 1987).

For example, for a reaction rate $R = k[A]$, the rate constant in conventional transition state theory is given by

$$k = \frac{k_B T}{h} \frac{q_\ddagger}{q_A} e^{-E_0/RT} \qquad (1)$$

where k_B is Boltzmann's constant, h is Planck's constant, T is the Kelvin temperature, and R is the gas constant. The first factor of Eq. 1 has the dimensions of frequency. (The factor if 6×10^{12} at 300K). The second factor is a ratio of partition functions per unit volume, with $q_\ddagger$ being the partition function of the activated state not including the single reaction coordinate. The energy E_0 is the molar energy change at 0 K when species A reacts from its thermodynamic standard state. It is important to notice that no structural information appears in Eq. 1. To make calculations with Eq. 1 requires knowledge of the structure-dependent potential energy surface of the system, which is only able to be formulated for relatively simple molecules.

While Eq. 1 in concept could be applied to the transitions of polymer channels, the practical outcome is that it cannot. However, the general ideas can be adapted to a description of the reaction on a continuum of polymer conformations. Since the populations of various structural forms are relatively insensitive to temperature (widely different structures are within a few $k_B T$ [Widom, 1965, 1975; Clementi, 1985]), we expect that the rate of the reaction will be limited by the probability of migrating to some narrow structural range of transition. This idea is formulated more concretely next.

Calculations and simulations of the structural motion

One way to carry out mathematical calculations for the time dependence of the migration of some molecule fragment on a bounded continuum involves a complicated descriptive equation. For instance, when there is a constant field (linear potential drop) over a bounded continuum, two distinct general mathematical forms arise when describing such diffusion in space (Carslaw and Jaeger, 1959). Both are infinite series: one is a series of time exponentials and the other is a series of complimentary error functions. Neither of the two series converges rapidly outside of its appropriate, limited time frame.

In a second approach, such a random walk can be simulated with a carefully chosen random number generator (Park and Miller, 1988), and a sufficient number of jumps can be made to obtain a smooth curve to mimic the time dependence for the round trip.

However, a straightforward and efficient probability simulation can be devised to replace both the infinite series and the simulated random walks. The calculation involves determining the time-dependent probabilities that the migrating structural unit(s) are located at sites that reside at a specific number of uniform steps from the transition region (see Fig. 1). A reflection at the barrier is modeled by a probability of unity that the next jump returns the structure unit back to the position from which it arrived. Once the structure passes the transition region, it is in the other chemical form, and so no reflections are allowed from that boundary; the transition region is, in effect, "absorbing." At the grid points between the reflecting barrier and the absorbing transition region, the total probability of being in a given position is the sum of probabilities of arriving from the two adjacent positions. In Fig. 1, the probabilities shown

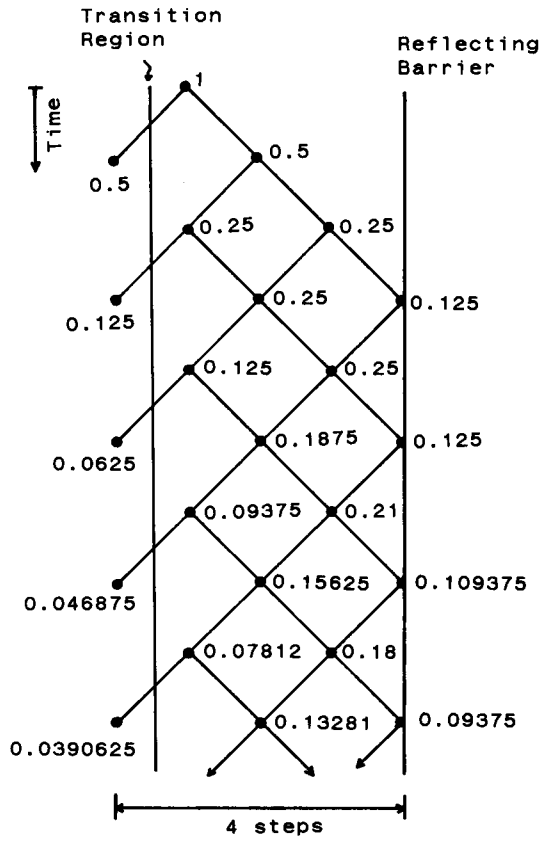

FIGURE 1 Illustration of the algorithm used to calculate the kinetics of first returns in a one-dimensional bounded continuum of conformations with a reflecting barrier that is an integral number of average jumps away from the transition region. Here, a barrier four jumps away is shown. The round trip diffusion represents migration of group(s) that are essential for the channel progressing from open to closed to open. The diffusing group passes the boundary between open/closed forms and then progresses by jumping at an average rate with probabilities p toward and q away from the transition region. At the reflecting boundary, the probability of reflection is unity. The probabilities labeled on the time-position grid are the results when $p = q = 0.5$. The conformation begins with unity probability, and, after one random jump, the probability of having left is 0.5. The probability of leaving at each average jump time is shown at the nodes at the left. Note how slowly the probability changes at the reflecting wall compared with the transition region. As a result, one may think of the conformations as "leaking" through the transition region. This is the origin of the first-order kinetics for these macromolecules. Any bias to the migration by a field interacting with the charged groups biases the motion over the entire range of distance.

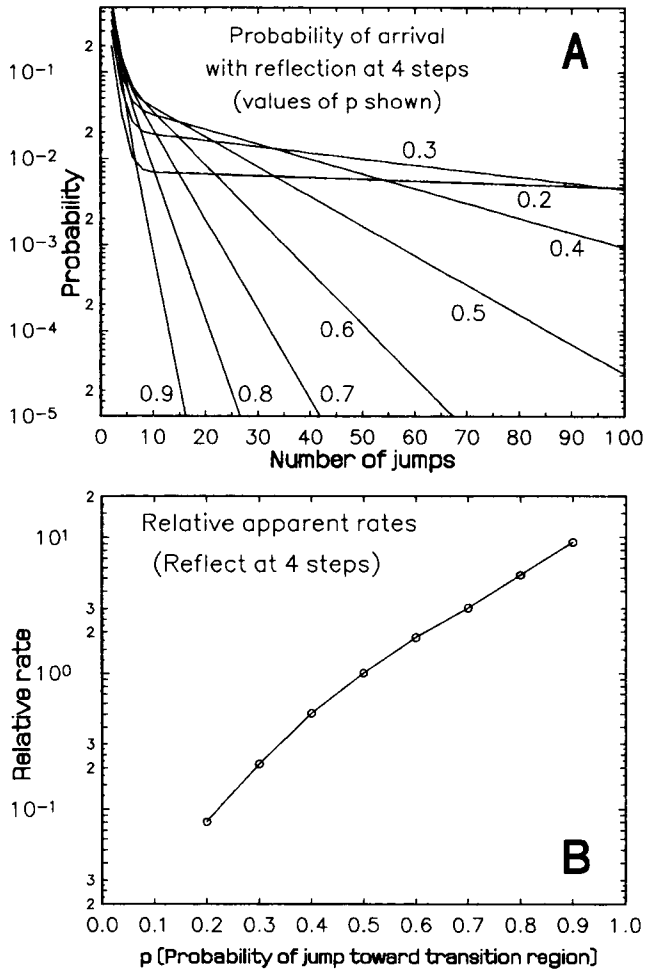

FIGURE 2 (A) Simulation of the probability of first returns versus time (time is measured by the number of jumps) for various biases. The bias is represented by different values of p, which are written adjacent to each curve. The reflecting barrier is assumed to be fixed at a distance of four average step lengths. As can be seen from this semi-logarithmic plot, the curves appear to become exponential relatively quickly. The apparent rate constants for these exponentials are plotted versus p in B, which is a semi-log plot of the relative rate versus bias. If we expect the bias to be linearly proportional to the electric field, the horizontal axis in B could be labeled "voltage" as well. The simulation suggests that the kinetics of first returns on a one-dimensional bounded continuum will appear with $(\mathrm{d} \log k/\mathrm{d}V) \approx$ constant. The rates are normalized to the rate of unity for $p = 0.5$, the unbiased walk.

at the leftmost grid points are the probabilities of arrival at the other structural form; this corresponds to the observable change in current in the single-channel experiments.

When no field is present to bias the motion, this probability of arrival appears as plotted in Fig. 2 A as the curve for $p = 0.5$. (The jump probability p is defined in the legend to Fig. 1.) The axes are semi-logarithmic, and, as can be seen, after an initial $t^{-3/2}$ drop, the probability of first returns decreases apparently exponentially. In other words, at short times the return might as well be occurring on a semi-infinite continuum (one boundary infinitely distant from an origin). However, at later times—when returns after reflections are possible—the time dependence of the transition probabilities becomes

exponential. This apparent first-order behavior originates, however, with a different mechanism from a rate that is limited by an activation enthalpy. Anticipating the result, we will find that the origin of the first-order behavior is analogous to a leak of gas through a hole in its container; the pressure decreases exponentially since the leak rate depends on the pressure of the remaining gas.

With these results in hand, let us list explicitly the assumptions used in making the calculation. (1) The random walk occurs in a region with a reflecting plane at some fixed distance, and "absorption" at the plane of the transition region. This absorption simply means that the channel's structure has shifted to the other form. In addition, we have assumed that (2) no inherent activation humps exist; in other words, there are no traps in the energy surface. (3) The jump lengths are all fixed at an average value. (4) The jumps all occur with the same average time interval between. (5) Reflecting boundaries lie at an integral number of average jump lengths from the structure(s) of the transition region. (6) Any bias (drift) in the random walk is uniform over the entire diffusion range, and the bias is proportional to the applied field. This last point is discussed further next.

How the rates are changed by electric fields

The apparent rates of reaction are expected to be changed by application of an electric field, which biases the diffusive random walk of ionic group(s) of the channel. A bias to the random walk is modeled simply by changing the values of the jump probabilities p and q appropriately; the resulting behavior is also shown in Fig. 2 *A*. In Fig. 2 *B* we plot the effective rates of the exponential portions of the curves against p. Since $p \propto V$, we thus obtain an approximation of the expected voltage-dependent changes in the first-order rates. It should be clear from Fig. 2 *B* that it would be difficult indeed to differentiate this voltage dependence of the first-order polymer migration kinetics from the usual Nernstian behavior for small-molecule kinetics, e.g., at electrodes, which shows $\mathrm{d} \ln k/\mathrm{d}V = \text{constant}$.

Mathematical description: the geometric distribution

The exponential kinetics in the polymer continuum can be described by a limiting form of the mathematical geometric distribution. The Geometric distribution is applied in the following circumstances. A series of independent trials is observed where the probability of success at each trial remains constant at s. (The value of s will be related to the probability of the channel passing successfully through the transition region to the other form.) The probability of failure (i.e., reflection) is denoted $f = (1 - s)$. The independent trials are continued until exactly one success has occurred.

After randomly migrating among the conformations of one form (closed or openable), the channel occasionally reaches the transition region with an average rate of arrival of ξ per second. Then the total average number of trials is ξt, and the Geometric distribution yields the time dependence of a single molecule changing its form:

$$\rho(\xi t; s) = s f^{\xi t}. \tag{2}$$

For a population with initial concentration $[A]_0$, the rate equation is then

$$[A]_t = [A]_0 s f^{\xi t}. \tag{3}$$

We can compare Eq. 3 with the integrated first-order rate equation $[A]_t = [A]_0 \exp(-k t)$ and find

$$\ln(e^{-kt}) - \ln(s f^{\xi t}). \tag{4}$$

Then,

$$-k t = \xi t \ln f + \text{constant}. \tag{5a}$$

Since the constant is of the order unity, we can write,

$$-k \approx \xi \ln f \tag{5b}$$

after a few trials. Here $\frac{1}{2} \leq f \leq 1$ and ξ is always positive; k is the rate constant. Eq. 5b shows that apparent first-order behavior is to be expected even for conformational interconversions when the energy barriers are essentially nonexistent. (In the small-molecule limit, a high activation energy means that the value of f approaches unity and ξ approaches vibrational frequencies.)

How the rates are changed by random thermal motions

As for all macromolecules, the molecules surrounding the channel are randomly colliding with it. As a result, the macromolecule's ability to occupy various parts of the surrounding regions is expected to fluctuate, and, consequently, varies the space within which various parts of the channel can migrate. Here, the changing spatial limit is modeled as a modulation of the position of the reflecting barrier. Changes in the distance to the reflecting barrier, in turn, modify the channel's apparent rate of transformation in a manner described next.

A probability calculation like that illustrated in Fig. 1 can be made for the first return times as they change with the distance between the reflecting barrier and the transition region. In Fig. 3, *A–C* are presented the PDFs calculated for first returns (different values of p) when the barriers are at 4, 6, 8, and 10 average jump distances. We see in Fig. 3 *D* that at the various fixed p (fixed drift

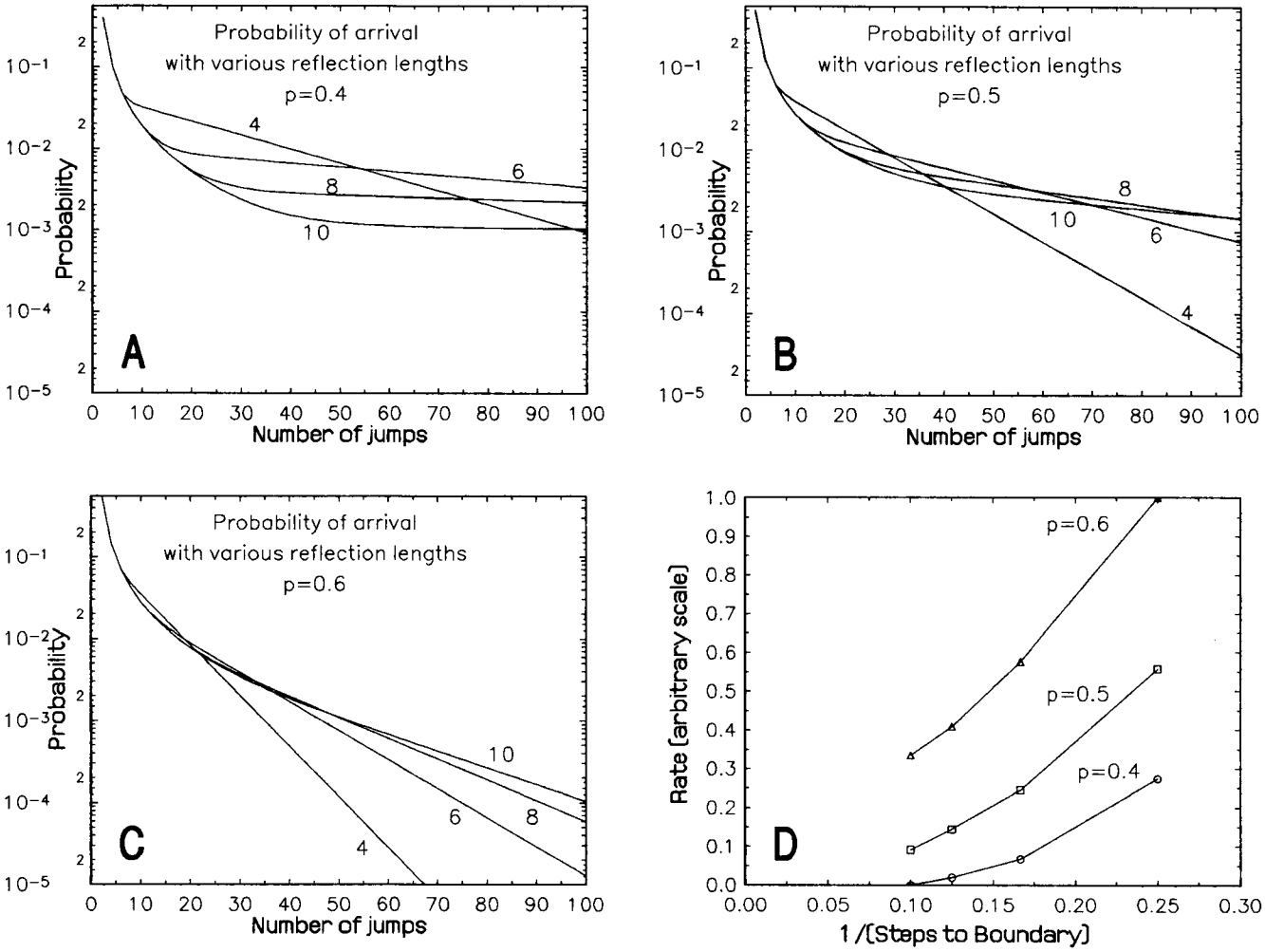

FIGURE 3 (*A–C*) Semi-log plots of the simulated first-return kinetics with varying distances to the reflecting barrier in a one-dimensional walk. As in Fig. 2, after an initial $t^{-3/2}$ decrease, the curves become exponential. In *D* are plotted three curves (one for each bias) of the relative apparent first-order rates of the exponential parts of the curves of *A–C*. The rates are plotted versus the inverse of the distance from the transition region to the reflection boundary since they are expected to be approximately proportional to that inverse distance.

in the field) the apparent rates of first returns change nearly linearly with the inverse of distance. Why does this occur? For the channel, the probability of reaching the transition region is higher when the essential structural unit(s) cannot migrate as far away. As a result, the available migration distance is then *inversely* proportional to a probability of being at the transition region. (For two- or three-dimensional diffusions, the average probability depends inversely on the available area or volume, respectively.) Again the analogy with a leak in a gas container can be invoked; when the barrier is closer, the pressure of a given quantity of gas is higher, and the leak faster.

The inverse relationship is presented pictorially in Fig. 4 *A*. This simplified model indicates that when the random thermal motion modulates the distance, the kinetic rate is expected to be modulated as well. A random modulation of distance is expected to show a Gaussian distribution in the positions of the reflecting boundary. This in turn causes a distribution of rates that is approximately Gaussian, and shows the physical origin of Eq. 9, which appears below. Eq. 9 is used here to fit the single-channel PDFs. The distribution of rates has the effect of producing a "tail" in the PDF.

Other viewpoints on the origins of tailed (or stretched) exponentials

Different continuous distributions of exponentials have been used numerous times in relaxation in condensed phases (Helfand, 1984; Adelman, 1986; Fröhlich, 1986;

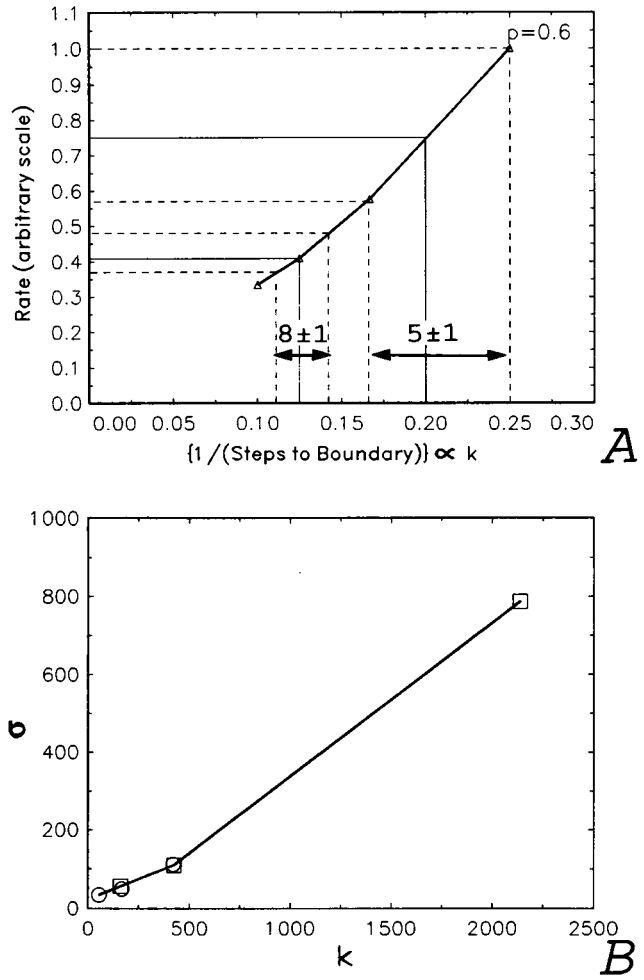

FIGURE 4 (*A*) Illustration of how the moldulation of distance is expected to produce a modulation of the apparent rate constant for round trip kinetics on a bounded continuum. Random thermal molulation of the boundary distances (horizontal axis) should produce a Gaussian distribution of displacement about the mean value. This, in turn, produces a Gaussian distribution of rates (vertical axis). The diagram also illustrates roughly why the experimental value of σ is expected to increase monotonically with an increase in the average rate constant $\bar{k}$. The values 5 ± 1 and 8 ± 1 indicate the number of steps between the reflecting barrier and the transition region. As indicated, the shorter the distance accessible, the larger the spread of rates for a given change in distance. For the round trip kinetics on a continuum, the value of (1/steps to boundary) is expected to be proportional to the apparent rate $\bar{k}$, but the value of σ is also dependent on the same quantity. (*B*) Plot of σ versus $\bar{k}$ as found from data fits with Eq. 9: ○ from the open-form PDFs and □ from the closed-form PDFs. The overlay of the middle two sets of points indicates that the open- and closed-form PDFs are congruent. The lines connecting the points are present only to show the trend.

Ehrenberg, 1987). Perhaps the clearest earlier examples of rate distributions in polymers is seen in the work of Schaefer and his co-workers. (Schaefer and Nautsch, 1972; Schaefer, 1973; Schaefer et al., 1977). A vast literature of the theory of tailed, nonexponential kinetics and a broad variety of approaches have been made to explain how they arise for apparently simple reactions (Vineyard, 1957; Williams and Watts, 1970; Bordewijk, 1975; Grassberger and Procaccia, 1982; Montroll and Shlesinger, 1982; Torell, 1982; Rajagopal et al., 1983; Palmer et al., 1984; Shlesinger and Montroll, 1984; Ngai et al., 1985; Klafter and Shlesinger, 1986; Plonka, 1986, 1989; Skolnick et al., 1987). The phenomenon appears over a wide range of molecular sizes and times: from small molecules in the picosecond time range up to the ion channels with millisecond kinetics (Jonscher, 1977).

Even though the local molecular environment always fluctuates, it is generally agreed that the effects are only revealed experimentally when the fluctuations occur within the same time scale as the observed kinetics (Simha, 1942; Havriliak and Negami, 1966, 1967; Hedvig, 1977; Dissado and Hill, 1979; Skinner, 1983). For the model developed here, the fluctuations in the distance to reflection that influence the rates must be in the micro- to millisecond range. If the time scales of the kinetics and environmental fluctuations are significantly different, then an experiment will measure averages of rates; the tail disappears and an exponential population decrease (or increase) results. For example, for numerous polymers the tailed conformational relaxations can be converted to a simple exponential form by changing the temperature at which the experiment is done (Jonscher, 1977; Ferry, 1980; Alkanis and MacKnight, 1983; Helfand, 1984). Usually, the temperature is elevated from a glass transition or from a freezing point if no glass forms. Similar phenomena may be expected from the ion channels.

To explain the tails within the conventional activated state theory, Macdonald (1962) delineates the requirements and difficulties of finding valid descriptions of broadened relaxations in thermally activated systems. He asserts that the temperature independence of the probability density of the activation energies (assuming temperature-independent frequency factors) constitutes a test of a valid distribution function of rate constants. One distribution that fits the criterion in many cases is a log-normal probability density of relaxation times that results from a Gaussian distribution of activation energies. When the log-normal distribution appears to be temperature dependent, a distribution of the power function type appears to be better. Macdonald (1962) suggests that a test also exists to check the correctness of the power function description: for a kinetic form given by $t^{(1+\rho)}$, ρ should be linearly dependent on temperature. This relationship may be useful in probing the fractal description of gating.

However, I suggest that the kinetics of the polymeric channels be described by a Gaussian distribution of

first-order rates, Eq. 9. Such an analysis is next applied to the single-channel PDFs of a bachtrachotoxin-treated sodium channel.

FITTING THE DATA CURVES WITH MATHEMATICAL ANALOGUE

Finding a decent curve fit to the single-channel PDF experimental data is a relatively easy exercise. Using contemporary computer tools, models of varying complexity can be formulated, the data fit well, and the voltage dependencies of the variables described. However, the quality of the fit is only one test of the quality of a model. Equally important are the parameters that describe and explain the voltage behavior of the variables. For example, if the graph of the logarithm of the rate (a variable) versus voltage is linear, the slope of the plot is characterizable with the parameter value of the charge of activation $\Delta z^{\ddagger}$ of the reaction. Such parameters exhibit certain simple behaviors, and numerous sets of parameters have straightforward interrelationships. As a result, having the parameters follow the expected behavior is a powerful test of the validity of a mathematical analogue.

The power of analysis using parameter behavior tests is that if the activated state chemical kinetics is assumed to apply to the interconversion of the various forms of the channel, then the rates can exhibit only a few possible voltage dependences, and each distinguishes a specific type of process (Rubinson, 1980). For example, if the rate changes linearly with voltage, the process results from conduction; if the rate change is logarithmic with voltage, the process is limited by a barrier; and if the rate change is quadratic with voltage, then it is due to second-order (dipolar) polarization phenomena. If one of these rate behaviors is not found, then a different reaction scheme probably should be tried or nonlinear changes in the internal electric field must be included.

For the data from single channels under steady-state conditions, the values of the variable $\bar{k}$ of Eq. 9 obtained from the best data fits are shown to agree with two parameter tests: (*a*) These phenomenological average rate constants follow the logarithmic dependence on voltage and, as expected (Audebert, 1947; Randles, 1952),

$$\frac{\mathrm{d} \log \bar{k}_{\text{opening}}}{\mathrm{d}V} \simeq -\frac{\mathrm{d} \log \bar{k}_{\text{closing}}}{\mathrm{d}V}. \tag{6}$$

(*b*) The forward and reverse rate constants are related to the equilibrium constant by the usual relationship,

$$K_{\text{eq}} = \frac{\bar{k}_{\text{opening}}}{\bar{k}_{\text{closing}}}, \tag{7}$$

which contains the inherent assumption of a transition between only two prevalent forms of the channel.

On the other hand, a number of multistate models of the single-channel kinetics exhibit rates that violate decisively the parameter tests: not only do the rate constants disagree quantitatively with the expectations for their behavior as described in Eq. 6, but in some cases their behavior violates the relationship of having opposite slopes as indicated by the negative sign in Eq. 6.

Data-fitting techniques

Data exhibiting long-tailed behavior such as the time-dependent PDFs for the sodium channel present formidable challenges in deciding how to determine what is the best mathematical analogue. Highly sophisticated statistics has been applied to such tailed data (Hall and Selinger, 1984; Alcala et al., 1987; Aubard et al., 1987; Livesey and Brochon, 1987; Yeramian and Claverie, 1987; Siemiarczuk et al., 1990). If the mathematical arguments alone could be clearly convincing, the debate would now be over.

Even without the uncertainties of distortion of the PDF shape by the bandwidth limitations (Colquhoun and Sigworth, 1983; Blatz and Magelby, 1986; Milne et al., 1989), the primary obstacles are familiar: minute misfits of shape or relatively small noise levels in the steep regions tend to dominate the statistics compared with the fitting of the more numerous points at regions of low slope. Also, the relative noise level of the data in the tail region tends to be larger than at earlier times, while the underlying physics and chemistry suggest that the tail is likely to be important to the physical description of the underlying process.

One impediment to testing the quality of fit is the inability to use one of the preferred techniques of statisticians: to linearize the data at all potentials in a simple way (Tukey, 1977). This problem has been partly overcome by a simultaneous data fitting and linearization scheme described by Liebovitch and Sullivan (1987), but the method is model specific.

The statistical function-fitting techniques with a single, global measure of quality of fit (Matheson, 1990) often produce best-fit curves that are, say, high over the first third of the time range, low over the second third, and high over the final third. In comparison, if we would draw a smooth best-fit curve by hand, we would most likely ensure that to the best of our ability the drawn line would have alternate data points above and then below it to provide a more localized best fit to the points. (Also see Knuth [1981] about the statistics of random number sequences.)

For the data fitting done for this work, the statistical and manual methods were joined. In Cartesian space,

the curve fits were tested by a nonlinear, least-squares minimization program that uses the Marquardt process. The data points and the calculated curve were then compared on a graph, and if the deviation of one early or midrange point contributed an excessive amount to the global error measure, it was removed so that the tail points would be better fit. If two curves were essentially identical in quality of fit, then the variables that were chosen were the ones providing a better fit to the tail region (if necessary, magnified as seen in Fig. 5). The better fit to the tail is defined as noted above, with the same number of data points above and below the line in the time range.

The least-squares program that was used is a transla-

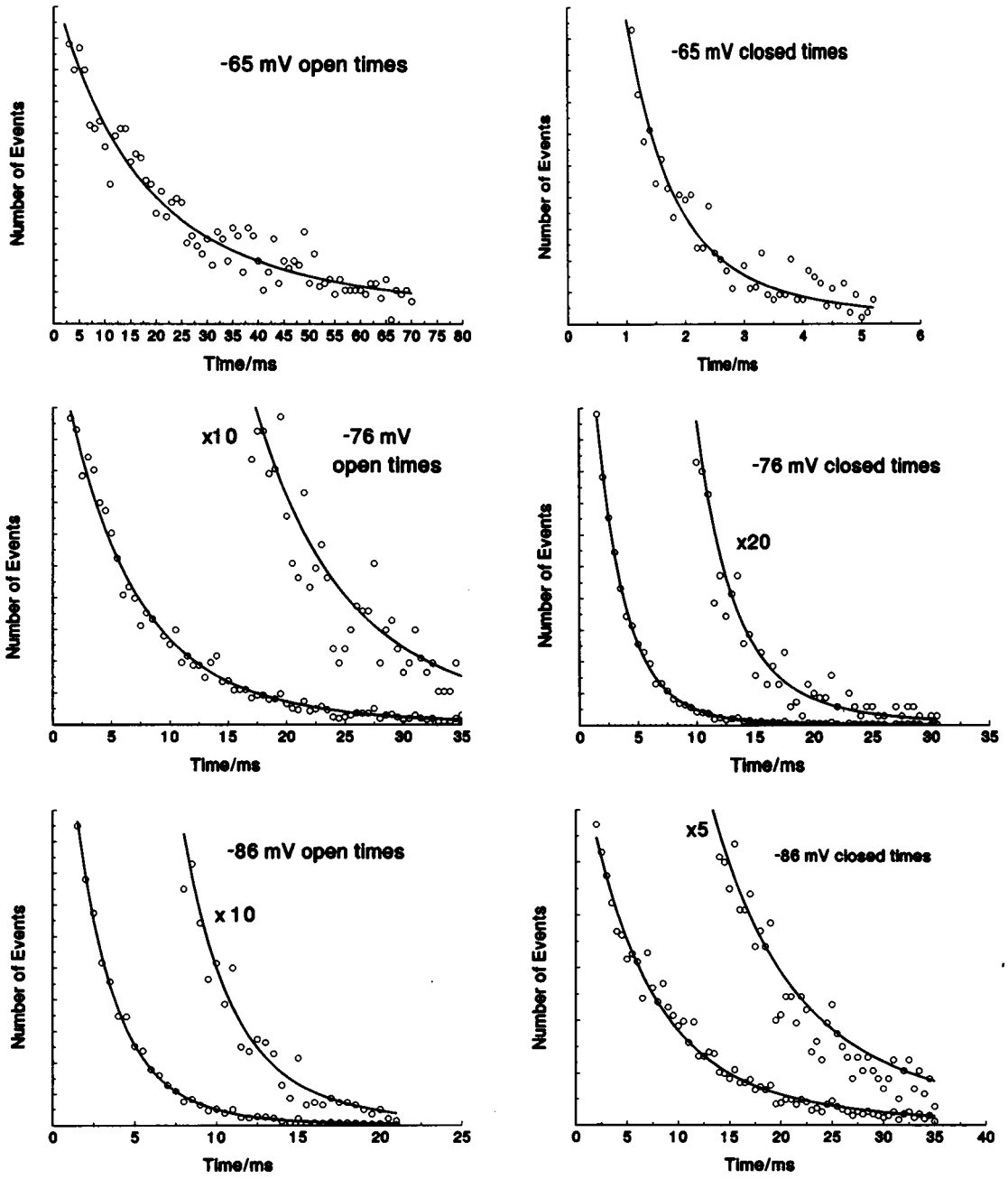

FIGURE 5 Fitting of the data with Eq. 9, a Gaussian distribution of exponentials. Data points are open circles with the calculated values plotted as a solid line. Y axis magnifications are noted at the appropriate curves.

tion into GW-BASIC of a Nottingham Algorithms Group (NAG) FORTRAN program (used with permission). A graphics output was added. The figures published here were drawn using AXUM™ version 1.02 (TriMetrix, Inc., Seattle, WA).

The PDFs from an experiment on a bachtrachotoxin-treated single sodium channel were generously provided by Bernard Keller and Mauricio Montal. The experimental details were published (Keller et al., 1986). Data at three potentials were provided (−65, −76, and −86 mV).

Equations

A number of different equations representing different mathematical analogues were tried in fitting the data. Among them were equations using power functions of the general type

$$\rho(t) = A \exp(-kt^n). \quad (8)$$

Exponentials and sums of exponentials were tried and rejected because of the lack of consistency with known chemistry and physics (see below). A large number of different equations that describe different models of diffusion of ionic groups (or holes) on a bounded continuum were tried. Examples are one-, two-, and three-dimensional diffusion with and without bias in semi-infinite and bounded spaces, all with various boundary conditions (such as absorbing boundaries) or with chemical reactions at some rate occurring, as appropriate, at planes, lines, and points. Most equations are detailed in Crank (1975) chapters 3, 4, and 14 and in Carslaw and Jaeger (1959) chapters 2, 3, and 10. However, other than Eq. 9, all were rejected since they either could not fit the PDFs well at all three potentials, or the parameters deriving from the fits were self-inconsistent. An example of self-inconsistent parameters is a contradiction of the directions of field-driven bias: for instance, the best-fit variables indicated that the open form was electrophoretically driven toward the closed form at the same time that the closed form was driven toward the open form. This is nonsense in a real physical system, and all such analogues were rejected.

By the test of least squares, a Gaussian distribution of exponentials produced better fits to all the curves than any of the other mathematical analogues tested. The Gaussian distribution of exponentials is given by

$$\rho(t) = A_0 \exp\left[-\left(\bar{k}t - \frac{\sigma^2 t^2}{2}\right)\right] \operatorname{erfc}\left[\frac{1}{\sqrt{2}}\left(\sigma t - \frac{\bar{k}}{\sigma}\right)\right], \quad (9)$$

which is derived in Appendix I. This equation has two kinetic variables: $\bar{k}$, the central or average apparent first-order rate constant, and σ, the standard deviation of the Gaussian distribution of apparent rate constants. The symbol erfc indicates the complementary error function, which is discussed further in Appendix I. The value A_0 is used to scale the amplitude to match the data curve. The curve fits are illustrated in Fig. 5. In Table I are shown the values of the kinetic variables for the best fits of the six data sets. The interpretation of the variables and parameters of Eq. 9 is presented in the Discussion. However, here we note that in addition to fitting the PDF data within experimental error, the mean apparent rate constants listed in Table I satisfied the parameter tests described by Eqs. 6 and 7.

Finally, we note that Eq. 9 can also act as a mathematically closed form substitute for a log-normal distribution of exponentials. The log-normal distribution has a larger probability density of faster rates, but it cannot fit these data better. The reason is that the earliest times of the PDFs—the region affected by faster rates—are not accessible because of the bandwidth limitations; changes in the faster rates are not seen. However, the fits of the PDFs by log-normal distributions of first-order rates were not as good as those of Eq. 9.

DISCUSSION: PARAMETERS AND PARAMETER INTERRELATIONSHIPS

Relationships of the voltage dependence of reaction rates

Within ion-containing systems such as the channels, the molecular motions associated with the measured kinetics may range over several ångströms, well beyond the distances of chemical bond formation in condensed phases. As discussed briefly in Appendix III, the rate *constants* are not expected to be strongly dependent on the potential even though the *rates* may change. The voltage-dependent change in the rates is expected to result from the electric field–dependent changes in local reactive concentrations.

The rate changes for the steady-state sodium channel appear to follow the behavior resulting from the kinetics of charges at interfaces: the rates change exponentially with potential, and the forward and reverse rates have

TABLE I Best-fitting kinetic variables of Eq. 9

	Closed-channel PDFs			Open-channel PDFs				
	$\bar{k}/s^{-1}$	σ/s^{-1}	$\bar{k}/\sigma$	$\bar{k}/s^{-1}$	σ/s^{-1}	$\bar{k}/\sigma$	K_{eq}	P_{open}
−65 mV	2,100	790	2.7	53	34	1.6	34	0.97
−76 mV	423	110	3.8	167	49	3.4	2.5	0.72
−86 mV	160	56	2.8	420	112	3.8	0.38	0.28

their slopes (i.e., $d[\ln \bar{k}]/dV$) that are approximately equal and opposite.[1] The best fits to the variables (shown in Table I) give slopes of −23.3 mV/decade and +20.0 mV/decade, which are equal within calculational error.

On the other hand, the rates found using the multiple- Markov–state formalism do not follow the behavior expected for first-order reactions (the behavior expressed in the fundamental relationship stated in Eq. 6). In fact, some of the sets of published forward and reverse rates have slopes $d(\ln k_{apparent})/dV$ with the same mathematical sign. (In that case, the slopes violate the symmetry properties of the membrane/channel system.) No scaling factors can rectify such a violation within the activated state formalism. One way to rationalize these violations is to assert that the field felt internally is not related linearly to the applied field. However, this assertion has not been part of such models. Accordingly, the multistate (Markovian) analogues for the channel kinetics are rejected since they fail at least one of the parameter tests.

Relating equilibria and rate constants

The chemical equilibrium constant and rates of a simple conformational equilibrium between two conformational states, e.g.,

$$A \underset{k_r}{\overset{k_f}{\rightleftharpoons}} B, \tag{10}$$

are related simply by $K_{eq} = k_f/k_r$. A similar simple expression—that stated in Eq. 7—might also be expected to hold for the average apparent first-order rate constants of the polymeric sodium channels. The parameter test of Eq. 7 is fulfilled if the following requirement is met: the spread of apparent rate constants must be consolidated (i.e., averaged) correctly by the distribution. (A corollary to this requirement is that the PDFs are, in fact, correctly described as a distribution of first-order reactions.) For a Gaussian distribution of rate constants, the consolidation is achieved by using the mean rate constant $\bar{k}$.

An experimental test of the validity of Eq. 9, then, is to compare the values of the equilibrium constants calculated directly from the experimental record of current versus time with the equilibrium constants calculated from the ratios of average apparent rates. This is done by comparing P_{open} calculated directly from the current records (Fig. 4 of Keller et al., 1986) with the values of P_{open} calculated from the ratios of the $\bar{k}$ values of Table I. The latter calculation is done using Eq. 11,

$$P_{open} = \frac{K_{eq}}{1 + K_{eq}}, \tag{11}$$

and both sets of P_{open} values are plotted in Fig. 6. The agreement is quite gratifying and infers that a Gaussian distribution of rates is a satisfactory mathematical analogue within the voltage range available.

Relating σ and $\bar{k}$

In Fig. 4*B* are plotted the best-fit values of σ, the standard deviations of the rate constants, versus $\bar{k}$, their associated mean rate constants for each open and closed channel PDF. The monotonic correlation between them is clear. This close relationship between $\bar{k}$ and σ is expected since both depend on the distance to the boundary. The relationship is illustrated qualitatively in Fig. 4*A*. We expect that the range of modulation is fixed by k_BT and the elasticity of the molecule. To approximate this situation, let us compare changing each effective barrier distance by unitary steps. Then the equivalent modulation of the rates corresponds to the

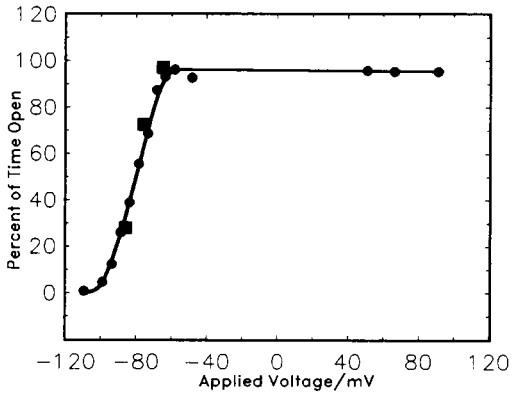

FIGURE 6 Redrawn plot of data (●) of P_{open} versus potential (from Keller et al., 1986) together with the values (■) of P_{open} calculated from the mean rate constants $\bar{k}$ using Eqs. 7 and 11. The agreement indicates that the Gaussian distribution adequately accounts for the spread of rates that appear.

[1]Three types of potential-dependent chemical processes are reasonably expected for the membrane systems, and the voltage dependence of the apparent rate constants differs for each type. These are: $(dk/dV) \propto V$ when the reaction results from charge movement by migration (conduction); $(d \ln k/dV) \propto V$ when the reaction involves charges at an interface; and $(d \ln k/dV) \propto V^2$ for dipolar (second-order) polarization (Rubinson, 1980). In the second case, when $[d \ln (\text{rate})/dV] \propto V$, changes in rate constant (as is true for electron transfer rates at electrode surfaces) are only expected when the majority of the field drop occurs over a few atomic diameters or less. For the polymers, we do not expect to see behavior of the type $(d \ln k/dV) \propto V^2$ because the local voltage drop is so small. A bond or group dipole does not subtend much of the field. (There may be an indirect effect of dipoles in which the bulk dielectric polarization changes the local internal field. This effect should follow Langevin behavior.)

distances between the sets of dashed lines in Fig. 4 *A*, where we note that the *relative* modulation of the rate is inversely related to the reflection distances. The observed, direct relationship between $\bar{k}$ and σ follows from this, since the magnitude of $\bar{k}$ is also inversely proportional to the barrier distance. The similar curvature of the curves in 4 *A* and *B*, may be accidental.

Bursts

The single-channel currents show the presence of periods of relatively rapid interconversion between open and closed forms separated by far longer periods in one form: the pattern referred to as bursts. We can equate this behavior to the well-known phenomenon in condensed-phase chemistry that is called the cage effect.[2]

The cage effect was first suggested in 1936 in a paper by Rabinowitch and Wood (1936; Rabinowitch, 1937). A mechanical model they constructed showed clustered collisions. From these results, they suggested that a simple reaction in a solvent differed from the same reaction in the gas phase: for fixed concentrations of reactants the presence of the solvent does not change the average number of collisions between molecules, but it does affect the time distribution of the collisions. The reagent collisions tend to occur in groups separated by extended periods without encounters.

Chemists envision that the reactants are prevented from colliding by intervening solvent molecules, and once the solvent is expelled, the reactants collide and the solvent holds them together making repeated contact within the solvent cage (Laidler, 1987). On the other hand, statisticians explain the groupings of the shorter periods of contact simply as the normal statistics of a random walk to a first return of the reactants (Feller, 1968). Within both the mathematical and chemical viewpoints, the ion channels in their steady state appear to provide a new experimental approach to investigate the cage effect.

Thus, the random walk on a bounded continuum may help provide a straightforward description of the basis of clustering of the short return times. When the molecule structure is spatially close to the transition region, it is more likely to return quickly and produce "bursts" when away from the transition region, it is more likely that the molecule residence times are long and produce the "tails" of the PDFs.

One usual assumption about the cage effect is that when the reactants escape the cage, the solvent again intervenes, and they no longer are reactive. The parallel assumption for the channel is that the average channel inactivation rate should be closely related to the escape time from the cage, since once the escape is made it is far less probable that the channel returns. Further, the cage effect's dependence on reactant mobility suggests that a longer burst duration is associated with a slower cage escape rate. This expectation appears to be fulfilled in experiments done by Nilius et al. (1989) on single sodium channels from guinea pig ventricular myocytes. In the presence of a chemical modifier that removes fast inactivation, but does not appear to change the open channel properties, they found a good, linear correlation of the inactivation time constant of the ensemble-average current with the burst duration.

The comparison of the channel with an elementary random walk inherently excludes the possibility that some activation enthalpy barriers may exist at the transition region. If an activation enthalpy barrier greater than a few k_BT is present, the probability of a transition is decreased: that is, s decreases and f increases. Eventually, when the activation enthalpy is large enough, the information of the time distribution of first returns of the random walk is lost. If the rate is controlled by an activation enthalpy, then the distribution of first-order rates passes over to log-normal because the rate distribution is determined by the modulation of the activation enthalpy and not the modulation of the arrival rate. Because of the bandpass limitations of single-channel data, we cannot eliminate the possibility that at least some activation enthalpy control may be present.

A peculiarity and some possible explanations

A most extraordinary finding of the experiments of Keller et al. (1986) is that even at the most positive voltages studied, the channel remained open no more than 95% of the time. The result is illustrated in Fig. 6. These data are unique and can only be obtained with this level of certainty from single-channel measurements in which the time dependence of the currents translates into an absolute fraction of the populations of the open and closed forms.

If further experiments show that the behavior arises from the properties of the polymer channel and is not strongly dependent on the solution ions, three chemically reasonable explanations arise when an interpretation is made within the continuum formalism: (1) The potential drop is significant at all points in the membrane, and the distances over which the channel remains in the open form are so narrow that the energy of interaction with the field cannot prevent the channel from migrating to the closed form. (2) The field drop is

[2]The verification of the cage effect is discussed by Noyes (1954, 1961), Grunwald et al. (1976), and Benesi, (1982). A general discussion is presented in Laidler (1987). A specific application to macromolecules was described by Keep and Pecora (1985).

not linear, and only a shallow potential gradient exists in the region where the conformations of the ionic groups allow an open channel. Again, the free energy needed to move from the reflecting barrier back to the transition region is too small to prevent the channel from proceeding to closed. (3) The charges that move in the field are neutralized to some degree by counter-charges in the region and render the field ineffective. In other words, counter-ions bind (ion pairing) to form a dipole which is significantly less affected by the field.

We can obtain a general idea of the free energy involved in this 95% open–time maximum. As an empirically determined limit, let us assume the channel is seen to be 100% open if $P_{open} = 0.999$, which is the equivalent of $K_{eq} = 1{,}000$. Similarly, $P_{open} = 0.95$ is equivalent to an equilibrium constant $K_{eq} = 19$. Since $\Delta G^0 = -RT \ln K_{eq}$, the free energy difference is in the range of only 3–4 k_BT. Of course these characteristics may be true only in the presence of batrachotoxin, and, thus, may have little relevance to normally operating channels.

EXPERIMENTAL TESTS

As narrated above, describing the PDFs as arising from a Gaussian distribution of first-order transformations has passed three tests: (*a*) The fits to the data are satisfactory; they are within experimental uncertainties. (*b*) The charge of activation (slopes of ln rate versus potential) is conserved. That is, Eq. 6 is satisfied. (*c*) The equilibrium constant is the quotient of the forward and reverse mean effective rates described by Eq. 7 and illustrated in Fig. 6.

Probes of the channel's characteristics and tests of the concepts of round trip kinetics involve experiments at the extremes of the voltage and temperature ranges of the system. The most important experiments involve the temperature dependence of the PDFs. Whether there is a change of shape in the PDFs and, if so, in what direction should be informative. For instance, if the temperature is lowered far enough, will it be possible to see the transition between $t^{-3/2}$ and exponential behavior at some potential, or will the broadening increase proportionally and still allow good fits with the distribution of exponentials?

If the early time $t^{-3/2}$ behavior can be discerned, then the mechanism of broadening can be tested. Since the conformations at the early, nonexponential, times do not involve reflection at the barrier, if the barrier distance modulation is responsible for broadening, we expect simple $t^{-3/2}$ behavior. However if migration rate modulation is responsible (either through viscosity fluctuations or field-shielding fluctuations), then the PDF at early times will be broadened as well.

The burst lengths are expected to decrease as the temperature is increased since the diffusion coefficient should increase, and both diffusion and electrophoresis are directly proportional to the diffusion rate. If at different temperatures the mean rate constants still provide good fits to the P_{open} equilibrium values, then this conservation should indicate the usefulness of the Gaussian distribution of exponentials as an analogue to describe the equilibrium and kinetics of steady-state channels. However, perhaps the most interesting result is to see whether P_{open} changes with temperature. If P_{open} fails to change, then the continuum model suggests that neither the field shape nor the relative extents of the open and closed forms are temperature dependent. Descriptive chemistry suggests that the extension should expand if enthalpic forces provide some contribution to the elastic effect, (Flory et al., 1959; Flory, 1961). However, if rubberlike elasticity is predominant, the extension is expected to be nearly temperature independent.

It remains to be seen whether the sodium channel's data agreement with the Gaussian distributed rates (Eq. 9) can be enlarged to provide a general principle for the kinetics of other biopolymers such as allosteric enzymes.

APPENDIX 1

In this appendix is derived the equation for a Gaussian distribution of exponentials. This description is imprecise and can be clarified by noting the analogy with a sum of two exponentials:

$$\rho(t) - A_1 e^{-k_1 t} + A_2 e^{-k_2 t}$$

The contribution of each of the two exponentials is denoted by the respective A_i values. In other words, the distribution refers to the amplitudes and not to the rate constants. In the continuum of conformations, we expect a continuum range of k_1 values. The maximum contribution is at a central (and mean) value $\bar{k}$. The function

$$\exp[-(\bar{k} + u)t] \qquad \text{(A1-1)}$$

expresses all the possible values of the rate constant, (i.e., $[\bar{k} + u]$) as u is allowed to vary from $-\bar{k}$ to infinitely large. The Gaussian distribution of contributions of the rates is given by

$$\frac{1}{\sigma\sqrt{2\pi}} \exp\left(-\frac{u^2}{2\sigma^2}\right). \qquad \text{(A1-2)}$$

The process of multipying Eqs. A1-1 and A1-2 point by point is that of convolution. The convolution integral is

$$\rho(t)/A_0 = \frac{1}{\sigma\sqrt{2\pi}} \int_{-\bar{k}}^{\infty} \exp\left(-\frac{u^2}{2\sigma^2}\right) \exp[-(\bar{k} + u)t]\, du. \qquad \text{(A1-3)}$$

A_0 is the scaling term to be used to fit the experimental curves. The exponents are collected, and a complete square can be formed by

adding and subtracting the term $\sigma^2 t^2/2$ to give

$$\rho(t)/A_0 = \frac{1}{\sigma\sqrt{2\pi}} \int_{-\bar{k}}^{\infty} \exp\left[-\left(\frac{[u + \sigma^2 t]^2}{2\sigma^2} + \bar{k}t - \frac{\sigma^2 t^2}{2}\right)\right] du, \quad \text{(A1-4)}$$

Because the integration is over u, the terms without u can be taken outside the integral. Next, the perfect square that remains in the exponent is substituted by w^2 to give

$$\rho(t)/A_0 = \frac{1}{2} \exp\left(-\bar{k}t + \frac{\sigma^2 t^2}{2}\right) \int_{\frac{-\bar{k}+\sigma^2 t}{\sigma\sqrt{2}}}^{\infty} \exp -w^2 \, dw. \quad \text{(A1-5)}$$

The integral is recognized as a complimentary error function of the form

$$\text{erfc}\,(z) = \frac{2}{\sqrt{\pi}} \int_z^{\infty} e^{-w^2} dw. \quad \text{(A1-6)}$$

Appropriate substitutions are made, and we arrive at the form of the equation that is used:

$$\rho(t) = A_0 \exp\left[-\left(\bar{k}\,t - \frac{\sigma^2 t^2}{2}\right)\right] \text{erfc}\left[\frac{1}{\sqrt{2}}\left(\sigma\,t - \frac{\bar{k}}{\sigma}\right)\right]. \quad (9)$$

The complimentary error function can be computed with an error limit of 3×10^{-7} with the numerical approximation 7.1.28 of Abramowitz and Stegun (1965).

APPENDIX 2

Characteristics of first returns in diffusional kinetics

When the transition region is chosen as the reference point within a continuum of conformations, the conformational migration then parallels a well-known problem in statistics, namely, the game in which two players flip coins for gain. In the game, the winner of a turn (e.g., one wins if the two match—if the coins show two heads or two tails) takes both coins. If the players both start with equal numbers of coins (parity) and flip at a regular rate, then, as the game progresses, one player takes the lead (has more than half the coins) for some time period and then the other one may lead. Between the switch of leader, the players must return to parity.

The sodium channel in the absence of a perturbing voltage can be related to this game in the following way. The transition region parallels the situation when both players have an equal number of coins. The regular flips are the jumps within the one-dimensional (or effectively one-dimensional) Brownian motion of the molecular group(s) essential to open the channel. The periods of time when one player is ahead in the game can be related to the time periods when the channel remains, say, open. In other words, the time required to complete a round-trip excursion from the transition region and back parallels the time at which the players again return to having equal numbers of coins for the *first* time after the game begins. (Since one player always takes the two coins, they have unequal numbers after the first flip.) One difference between the coin game and the sodium channels is that the channels' structural excursions are limited in extent. But, for the present, let us assume that the excursions are not limited in distance.

With this analogy of the single channel and the coin tossing game assumed, we can then apply the known stochastic properties of the game to the channel. These properties have been described in elegant detail by Feller (1968, especially pp. 75–76, 89, 273–275, and 356.) He shows how and under what conditions data from the single molecule observed over a prolonged time and collected into a histogram are *not* equivalent to data obtained from an ensemble of monodisperse channels being measured simultaneously under the same conditions over the time extent of the single-channel histogram.[3]

The basis for this difference is that more detailed information is obtained about the round trip of the single channel than is obtained about the ensemble of channels. To illustrate this difference, consider that an ensemble of particles resides in a homogeneous plane against a planar barrier infinite in extent. At time 0 the particles begin to diffuse without bias. The particles become distributed in the familiar time-dependent half-of-a-Gaussian distribution with the tail reaching away from the barrier. The time dependence of the concentration at the barrier surface is calculable from the diffusion equation evaluated at the origin; in this case the origin resides at the barrier surface. The concentration changes as $(1/\pi Dt)^{1/2}$, where D is the diffusion coefficient. The molecular processes that produce this time dependence involve some of the particles returning to the barrier and being reflected multiple times, and thus include numerous second returns, numerous third returns, etc.

If, in contrast, we use only one particle for the same diffusion experiment, we can register (and, within the bandwidth, we do so for the batrachotoxin-modified single channel) the times of each individual return to the barrier. Further, the clock is restarted at each return to calculate the PDF. Thus, when registering the returns, each is a *first* return. And, clearly, the average times that pass before a first return (after the previous return) are shorter than the average times to second, third, etc. returns. As discussed by Feller (1968), the probability of a first return goes as $(1/\pi Dt^3)^{1/2}$; that is, $t^{-3/2}$ rather than $t^{-1/2}$ for the ensemble.

Another oversimplified way to look at the difference between registering times of general returns and registering times of first returns is that the time elapsed before a general return is the integral of the time of first return: $t^{-1/2}$ is the time integral of $t^{-3/2}$. If no boundaries or bias were present, the first returns would decrease as $t^{-3/2}$ continuously. However, with a bounded diffusion range, the time course changes over to an apparently exponential decay after a time that depends on the distance limit to the boundary to further diffusion.

The analogy between the channel conformational migration and the coin-tossing game does not strictly hold if the motion is biased in one direction. Such bias is expected if an electric field influences the motions of charged groups. The effect of the field on a round trip in a bounded continuum is, perhaps, unexpectedly small since the field accelerates the drift in one direction, while in the opposite direction the drift is slowed by an equal speed.

[3]An interesting point made by Feller about the coin game is that the shape of the PDF of times between first returns to parity depends on the length of a game. Simply put, the longest "tail" that is measured (that which results from the longest time between returns to the starting balance) cannot be longer than the total length of the game. If a game is prolonged, then the tail of a PDF can be longer. There is a modest probability that one player will be ahead for the entire length of the game. This limiting model probably does not hold for the channels since the excursion distance from the starting point is limited. Modeling shows, however, that the results of an infinite excursion limit are little different from having a reflecting limit 50 steps from the transition region for an unbiased random walk. Further, experimentally it may be difficult to distinguish a random walk with a boundary 20 steps away from an unlimited random walk. For unbiased molecular jumps, the 20-step limit means that 3–5 Å is then experimentally "infinite."

APPENDIX 3

Local concentration dependence of reaction rates

In this appendix are shown the reasons why the voltage dependence of reactions in which the potential drop occurs over multi-ångström distances is due to changes in local concentrations rather than voltage-dependent changes in rate constants.

Refer to Fig. 7 *A*, which illustrates a common picture of the energy along the reaction coordinate versus position of an ion in passage through a channel. However, given the localized nature of bond formation, the changes in energy with binding to sites along the channel should be sharply limited in spatial extent as shown (*B*). We expect the traps to be on the order of a few ångströms wide, while the field drops over at least 30 Å. If the applied voltage drops even approximately linearly through the channel, then the applied voltage perturbs the rate constants only to a small extent. The reason is that the field drop across the reaction region (the trap) is expected to be only ~3–6% of the total transmembrane potential (1 Å/30 Å = 0.03). However, the rates can change significantly with voltage. A mechanism must exist to integrate the potential.

To be more specific, in the case for binding of some ion at a trapping site within an ion channel we write

$$\text{rate}_{\text{binding}} = k'_1\,[\text{ion}]_{\text{local}}[\text{site}]. \qquad \text{(A3-1)}$$

When written as a pseudo first-order equation, this becomes

$$\text{rate}_{\text{binding}} = k_1[\text{ion}]_{\text{local}}. \qquad \text{(A3-2)}$$

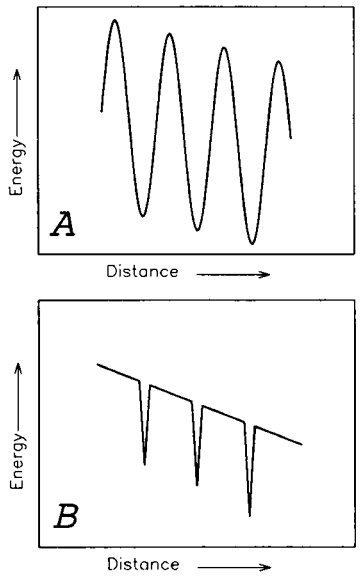

FIGURE 7 (*A*) An often-used activation energy diagram for an extended system. Here it is for transport of ions through a channel ~30 Å long. However, chemical bonds are formed and broken over distances of <1 Å. As a result, three sites for trapping ions would produce a one-dimensional reaction coordinate diagram such as is shown schematically in *B*. Ion concentration changes are expected to occur along the sloping regions, and it is such concentration changes that cause the rate changes with changing potential.

The site's activity (or concentration) is reflected in the new, unprimed rate constant. In the simplest case, the reacting ion may come from a bulk pool on one side of the membrane only. When the potential at the intrachannel site differs from the potential at the bulk by a fraction ϕ of ΔE, then Eq. A3-2 can be written in terms of an experimentally measurable ion concentration and transmembrane potential. At 300 K,

$$\text{rate}_{\text{binding}} = k_1[\text{ion}]_{\text{bulk}} \exp\,[\phi\,\Delta E\,z/0.026]. \qquad \text{(A3-3)}$$

Here z is the appropriate ionic charge of the mobile ion. The last term of Eq. A3-3 indicates the origin of the voltage dependence of the rate. It derives from the concentration gradient equivalent to the potential change. How can this behavior be proven? The answer lies in the reverse reaction—for the ion leaving the site. The reverse reaction's rate equation has the form

$$\text{rate}_{\text{leaving}} = k_{-1}[\text{ion} \cdot \text{site}]. \qquad \text{(A3-4)}$$

The form of Eq. A3-4 indicates that the rate of the reverse reaction is expected to be essentially independent of potential; the rate constant is expected to have a voltage dependence of only a few percent of the total potential, and there is no voltage dependence expected for the concentration of the site-bound ion that is spatially fixed.

As a result, a fundamentally different behavior is expected for a process where long distances and concentration-dependent rates are involved when compared with the rate processes at an electrode where the voltage does change the reaction-coordinate energy. In the usual-electrode processes, the voltage dependencies of the forward and reverse rates (log k versus ΔE) are approximately equal and opposite (Audebert, 1947; Randles, 1952). On the other hand, in the extended system the forward rate is expected to be voltage dependent to some extent, but the reverse rate should be voltage independent. This behavior is characteristic for the "long-distance" second-order binding reactions.

This characteristic behavior has indeed been observed experimentally for Mg^{2+} and Na^+ blocking of K^+ in potassium channels as measured by Horie et al. (1987). The block by both Mg^{2+} and Na^+ occurs at the same electrical distance, which implies the existence of the same binding site for both species.

This local concentration change by the voltage is extended to the first-order conformational changes of a channel by noting that changes in the rate at the transition region are caused by changing the populations of various conformations on the continuum. And the relatively large voltage dependencies of the rates are to a great extent due to relatively large changes in the time spent in locally reactive conformations and not to changes in various rate constants with potential.

The author would like to thank Darrell Fleishman, Gerald Alter, Ira Josephson, Larry Liebovitch, Larry Anderson, Larry Prochaska, and Richard Day for critically reading the manuscript and for helpful discussions. The PDF data were generously provided by Bernard Keller and Mauricio Montal.

Received for publication 7 December 1990 and in final form 30 September 1991.

REFERENCES

Abramowitz, M., and I. A. Stegun. 1965. Handbook of Mathematical Functions. Dover Publications, New York. 297–329.

Adelman, S. A. 1986. Some concepts in condensed phase chemical kinetics. *J. Stat. Phys.* 42:37–48.

Aklonis, J. J., and W. J. MacKnight. 1983. Introduction to Polymer Viscoelasticity. 2nd ed. John Wiley & Sons, Inc., New York. Chap. 3.

Alcala, J. R., E. Gratton, and F. G. Prendergast. 1987. Interpretation of fluorescence decays in proteins using continuous lifetime distributions. *Biophys. J.* 51:925–936.

Aubard, J., P. Levoir, A. Denis, and P. Claverie. 1987. Direct analysis of chemical relaxation signals by a method based on the combination of Laplace transform and Padé approximants. *Comput. & Chem.* 11:163–178.

Audebert, R. 1947. The theory of overvoltage. *Disc. Farad. Soc.* 1:72–80.

Benesi, A. J. 1982. Theory of elementary bimolecular reactions in liquid solutions. 1. Time spacing of recollisions between nonreactive molecules in liquid solutions. *J. Phys. Chem.* 86:4926–4930.

Blatz, A. L., and K. L. Magleby. 1986. Correcting single channel data for missed events. *Biophys. J.* 49:967–980.

Bordewijk, P. 1975. Defect-diffusion models of dielectric relaxation. *Chem. Phys. Lett.* 32:592–596.

Bruice, T. C. 1970. Proximity effects and enzyme catalysis. *In* The Enzymes. Vol. 2. 3rd ed. P. D. Boyer, editor Academic Press, New York. 217–279.

Canavos, G. C. 1984. Applied Probability and Statistical Methods. Little, Brown and Company, Boston. 94–102.

Carslaw, H. S., and J. C. Jaeger. 1959. Conduction of Heat in Solids. 2nd ed. Clarendon Press, Oxford. 50–91.

Clementi, E. 1985. Ab initio computational chemistry. *J. Phys. Chem.* 89:4426–4436.

Colquhoun, D., and F. J. Sigworth. 1983. Fitting and statistical analysis of single-channel records. *In* Single-Channel Recording. B. Sakmann and E. Neher, editors. Plenum Publishing Corp., New York. 191–263.

Crank, J. 1975. The Mathematics of Diffusion. 2nd ed. Clanendon Press, Oxford.

Croxton, T. L. 1988. A model of the gating of ion channels. *Biochim. Biophys. Acta.* 946:19–24.

Dickinson, E. 1985. Brownian dynamics with hydrodynamic interactions: the application to protein diffusional problems. *Chem. Soc. Rev.* 14:421–455.

Dissado, L. A., and R. M. Hill. 1979. Non-exponential decay in dielectrics and dynamics of corelated systems. *Nature (Lond.).* 279:685–689.

Dunitz, J. D. 1979. X-Ray Analysis and the Structure of Organic Molecules. Cornell University Press, Ithaca, NY. 301–390.

Ehrenberg, A. 1987. Viscosity and glycerol effects on dynamics of Cytochrome c. *In* Structure, Dynamics and Function of Biomolecules. A. Ehrenberg, R. Rigler, A. Gräslund, and L. Nilsson, editors. Springer-Verlag, Berlin. 43–46.

Eisenberg, R. S. 1990. Channels as enzymes. *J. Membr. Biol.* 115:1–12.

Feller, W. 1968. An Introduction to Probability Theory and Its Applications. Vol. I. 3rd ed. John Wiley & Sons, Inc., New York. 67–97.

Ferry, J. D. 1980. Viscoelastic Properties of Polymers. John Wiley & Sons, Inc., New York. Chap. 11.

Flory, P. J. 1961. Thermodynamic relations for high elastic materials. *Trans. Farad. Soc.* 57:829–838.

Flory, P. J. 1969. Statistical Mechanics of Chain Molecules. John Wiley & Sons, Inc., New York.

Flory, P. J., C. A. J. Hoeve, and A. Ciferri. 1959. Influence of bond angle restrictions on polymer elasticity. *J. Polym. Sci.* 34:337–347.

Fröhlich, H. 1986. Coherent excitation in active biological systems. *In* Modern Bioelectrochemistry. F. Gutmann and H. Keyzer, editors. Plenum Publishing Corp., New York. 241–261.

Gol'danskii, V. I., Yu. F. Krupyanskii, and V. N. Fleurov. 1986. Rayleigh scattering of Mössbauer radiation (RSMR) data, hydration effects and glass-like dynamical model of biopolymers. *Physica Scripta.* 33:527–540.

Grassberger, P., and I. Procaccia. 1982. The long time properties of diffusion in a medium with static traps. *J. Chem. Phys.* 77:6281–6284.

Grunwald, E., K. C. Chang, and J. E. Leffler. 1976. Effects of molecular mobility on reaction rates in liquid solutions. *Annu. Rev. Phys. Chem.* 27:369–385.

Hall, P., and B. Selinger. 1984. Better estimates of multiexponential decay parameters. *Zeitschrift für Physikalische Chemie Neue Folge.* 141:77–89.

Havriliak, S., and S. Negami. 1966. A complex plane analysis of α-dispersions in some polymer systems. *J. Polym. Sci. Part C.* 14:99–117.

Havriliak, S., and S. Negami. 1967. A complex plane representation of dielectric and mechanical relaxation processes in some polymers. *Polymer (London).* 8:161–210.

Hedvig, P. 1977. Dielectric Spectroscopy of Polymers. John Wiley & Sons, Inc., New York. Chaps. 1 and 2.

Helfand, E. 1984. Dynamics of conformational transitions in polymers. *Science (Wash. DC).* 226:647–650.

Horie, M., H. Irisawa, and A. Noma. 1987. Voltage-dependent magnesium block of adenosine-triphosphate-sensitive potassium channel in guinea-pig ventricular cells. *J. Physiol. (Lond.).* 387:251–272.

Jencks, W. P. 1969. Catalysis in Chemistry and Enzymology. McGraw-Hill Inc., New York. Chap. 1.

Jonscher, A. K. 1977. The 'universal' dielectric response. *Nature (Lond.).* 267:673–679.

Keep, G. T., and R. Pecora. 1985. Reevaluation of the dynamic model for rotational diffusion of thin, rigid rods in semidilute solution. *Macromolecules.* 18:1167–1173.

Keller, B. U., R. P. Hartshorne, J. A. Talvenheimo, W. A. Catterall, and M. Montal. 1986. Sodium channels in planar lipid bilayers. Channel gating kinetics of purified sodium channels modified by batrachotoxin. *J. Gen. Physiol.* 88: 1–23.

Klafter, J., and M. F. Shlesinger. 1986. On the relationship among three theories of relaxation in disordered systems. *Proc. Natl. Acad. Sci. USA* 83:848–851.

Knuth, D. I. 1981. The Art of Computer Programming. 2nd ed. Addison-Wesley Publishing Company, Reading, MA. 59–113.

Laidler, K. J. 1987. Chemical Kinetics. Harper & Row Publishers, Inc., New York. 187–188.

Läuger, P. 1988. Internal motions in proteins and gating kinetics of ionic channels. *Biophys. J.* 53:877–884.

Liebovitch, L. S. 1989. Testing fractal and Markov models of ion channel kinetics. *Biophys. J.* 55:373–377.

Liebovitch, L. S., and J. M. Sullivan. 1987. Fractal analysis of a voltage-dependent potassium channel from cultured mouse hippocampal neurons. *Biophys. J.* 52:979–988.

Liebovitch, L. S., J. Fischbarg, and J. P. Oniarek. 1987. Ion channel kinetics: a model based on fractal scaling rather than multistate Markov processes. *Math. Biosci.* 84:37–68.

Livesey, A. K., and J. C. Brochon. 1987. Analyzing the distribution of decay constants in pulse-fluorimetry using the maximum entropy method. *Biophys. J.* 52:693–706.

Macdonald, J. R. 1962. Restriction on the form of relaxation-time distribution functions for a thermally activated process. *J. Chem. Phys.* 26:345–349.

Matheson, I. B. C. 1990. A critical comparison of least absolute deviation fitting (robust) and least squares fitting: the importance of error distributions. *Comput. Chem.* 14:49–57.

Millhauser, G. L. 1990. Reptation theory of ion channel gating. *Biophys. J.* 57:857–864.

Millhauser, G. L., E. E. Salpeter, and R. E. Oswald. 1988. Diffusion models of ion-channel gating and the origin of power-law distributions from single-channel recording. *Proc. Natl. Acad. Sci. USA.* 85:1503–1507.

Milne, R. K., G. F. Yeo, B. W. Madsen, and R. O. Edeson. 1989. Estimation of single channel kinetics parameters from data subject to limited time resolution. *Biophys. J.* 55:673–676.

Montroll, E. W., and M. F. Shlesinger. 1982. On $1/f$ noise and other distributions with long tails. *Proc. Natl. Acad. Sci. USA.* 79:3380–3383.

Ngai, K. L., R. W. Rendell, A. K. Rajagopal, and S. Teitler. 1985. Three coupled relations for relaxations in complex systems. *Ann. NY Acad. Sci.* 484:150–184.

Nilius, B., J. Vereecke, and E. Carmeliet. 1989. Properties of the bursting Na channel in the presence of DPI 201-106 in guinea-pig ventricular myocytes. *Pflügers Arch. Eur. J. Physiol.* 413:234–241.

Noda, M., S. Shimizu, T. Tanabe, T. Takai, T. Kayano, T. Ikeda, H. Takahasi, H. Nakayama, Y. Kanaoka, N. Minamino et al. 1984. Primary structure of *Electrophorus electricus* sodium channel deduced from cDNA sequence. *Nature (Lond.).* 312:121–127.

Noyes, R. M. 1954. A treatment of chemical kinetics with special applicability to diffusion controlled reactions. *J. Chem. Phys.* 22:1349–1358.

Noyes, R. M. 1961. Effects of diffusion rates on chemical kinetics. *Prog. React. Kinet.* 1:129–160.

Palmer, R. G., D. L. Stein, E. Abrahams, and P. W. Anderson. 1984. Models of hierarchically constrained dynamics for glassy relaxation. *Phys. Rev. Lett.* 53:958–961.

Park, S. K., and K. W. Miller. 1988. Random number generators: Good ones are hard to find. *Commun. ACM.* 31:1192–1201.

Plonka, A. 1986. Time-Dependent Reactivity of Species in Condensed Media. Springer-Verlag, Berlin.

Plonka, A. 1989. ESR studies on reactivity of radiation produced species in condensed media. *In* Magnetic Resonance and Related Phenomena. J. Stankowski, N. Pistewski, S. K. Hoffman, S. Idziak, editors. Elsevier Science Publishers B.V., Amsterdam. 593–599.

Rabinowitch, E. 1937. Collision, co-ordination, diffusion, and reaction velocity in condensed systems. *Trans. Farad. Soc.* 33:1225–1233.

Rabinowitch, E., and W. C. Wood. 1936. The collison mechanism and the primary photochemical process in solutions. *Trans. Farad. Soc.* 32:1381–1387.

Rajagopal, A. K., K. L. Ngai, R. W. Rendell, and S. Teitler. 1983. Nonexponential decay in relaxation phenomena. *J. Stat. Phys.* 30:285–292.

Randles, J. E. B. 1952. Kinetics of rapid electrode reactions. II. Rate constants and activation energies of electrode reactions. *Trans. Farad. Soc.* 48:828–832.

Rubinson, K. A. 1978. Statistical triggering: a new way of looking at sigmoidal kinetics of voltage-dependent ionic channels. *J. Physiol. (Lond.)* 281:14P–15P.

Rubinson, K. A. 1980. Voltage dependencies of slow (msec) chemical relaxations. *Biophys. Chem.* 12:51–55.

Rubinson, K. A. 1982. The sodium currents of the nerve under voltage clamp as heterogeneous kinetics: a model that is consistent with possible kinetic behavior. *Biophys. Chem.* 15:245–262.

Rubinson, K. A. 1986*a*. The effects of *n*-pentane on voltage clamped squid nerve sodium currents: a reinterpretation using the kinetics of ordered systems. *Biophys. Chem.* 25:43–55.

Rubinson, K. A. 1986*b*. Closed channel-open channel equilibrium of the sodium channel of nerve: simple models of macromolecular equilibria. *Biophys. Chem.* 25:57–72.

Schaefer, J. 1973. Distributions of correlation times and the carbon-13 nuclear magnetic resonance spectra of polymers. *Macromolecules.* 6:882–888.

Schaefer, J., and D. F. S. Nautsch. 1972. Carbon-13 Overhauser effect in polymer solutions. *Macromolecules.* 5:416–427.

Schaefer, J., E. O. Stejskal, and R. Buchdahl. 1977. Magic-angle ^{13}C–NMR analysis of motion in solid glassy polymers. *Macromolecules.* 10:384–405.

Shlesinger, M. F., and E. W. Montroll. 1984. On the Williams-Watts function of dielectric relaxation. *Proc. Natl. Acad. Sci. USA.* 81:1280–1283.

Siemiarczuk, A., B. D. Wagner, and W. R. Ware. 1990. Comparison of the maximum entropy and exponential series methods for the recovery of distributions of lifetimes from fluorescence lifetime data. *J. Phys. Chem.* 94:1661–1666.

Simha, R. 1942. On relaxation effects in amorphous media. *J. Appl. Phys.* 13:210–207.

Skinner, J. L. 1983. Kinetic Ising model for polymer dynamics: applications to dielectric relaxation and dynamic depolarized light scattering. *J. Chem. Phys.* 79:1955–1964.

Skolnick, J., A. Kolinski, and R. Yaris. 1987. Monte Carlo studies of the long-time dynamics of dense polymer systems: the failure of the reptation model. *Accounts of Chem. Res.* 20:350–356.

Torell, L. M. 1982. Brillouin scattering study of hypersonic relaxation in a $Ca(NO_3)_2$-KNO_3 mixture. *J. Chem. Phys.* 76:3467–3473.

Tukey, J. W. 1977. Exploratory Data Analysis. Little, Brown and Company, Boston. Chaps. 4 and 6.

Vineyard, G. H. 1957. Frequency factors and isotope effects in solid state rate processes. *J. Phys. Chem. Solids.* 1957:121–127.

Widom, B. 1965. Molecular transitions and chemical reaction rates. *Science (Wash. DC).* 140:1555–1560.

Widom, B. 1971. Reaction kinetics in stochastic models. *J. Chem. Phys.* 55:44–52.

Williams, G., and D. C. Watts. 1970. Non-symmetrical dielectric relaxation behaviour arising from a simple empirical decay function. *Trans. Farad. Soc.* 66:80–85.

Yeramian, E., and P. Claverie. 1987. Analysis of multiexponential functions without a hypothesis as to the number of components. *Nature (Lond.).* 326:169–174.